

1 Microbial anodic consortia fed with fermentable substrates in  
2 microbial electrolysis cells: significance of microbial structures

3 Clément Flayac, Eric Trably, Nicolas Bernet

4 *LBE, Univ Montpellier, INRA, 102 avenue des Etangs, 11100 Narbonne, France*

5

6 ABSTRACT

7 Microbial community structure of anodic biofilms plays a key role in bioelectrochemical  
8 systems (BESs). When ecosystems are used as inocula, many bacterial species having  
9 interconnected ecological interactions are present. The aim of the present study was to  
10 identify these interactions for the conversion of single substrates into electrical current. Dual-  
11 chamber reactors were inoculated with activated sludge and fed in batch mode with acetate,  
12 lactate, butyrate and propionate at 80 mM<sup>e-</sup> equivalents in quadruplicate. Analyses of biofilms  
13 and planktonic microbial communities showed that the anodic biofilms were mainly  
14 dominated by the *Geobacter* genus (62.4 % of the total sequences). At the species level,  
15 *Geobacter sulfurreducens* was dominant in presence of lactate and acetate, while *Geobacter*  
16 *toluenoxydans* and *Geobacter pelophilus* were dominant with butyrate and propionate as  
17 substrates. These results indicate for the first time a specificity within the *Geobacter* genus  
18 towards the electron donor, suggesting a competitive process for electrode colonization and  
19 the implementations of syntrophic interactions for complete oxidation of substrates such as  
20 propionate and butyrate. All together, these results provide a new insight into the ecological  
21 relationships within electroactive biofilms and suggest eco-engineering perspectives to  
22 improve the performances of BESs.

23

24 *Keywords:* Anodic consortia – Microbial Electrolysis Cells – Fermentable substrates –  
25 Ecological relationships

## 26 **1 Introduction**

27         The massive use of fossil fuels has increased pollution with major climatic disruptions  
28 which implies the absolute necessity of developing renewable energies. New solutions need  
29 now to be considered to produce clean energy, and sustainable hydrogen is a good alternative  
30 for future transportation. Among the technologies able to generate H<sub>2</sub>, microbial electrolysis  
31 cells (MECs) constitute a very promising solution. In MEC, the organic matter contained in  
32 wastewaters is oxidized at the anode in CO<sub>2</sub>, electrons and protons by specific bacteria named  
33 electroactive bacteria (EABs). Electrons cross then the electrical circuit up to the cathode  
34 where they combine with protons to form hydrogen. This biological-assisted reaction requires  
35 a lower voltage (0.2-0.8 V) than water electrolysis (1.23-1.8 V) [1, 2]. Significant advances  
36 have been recently made to improve MECs performances through the increase of the current  
37 density (CD) and coulombic efficiency (CE), two essential parameters for future large-scale  
38 implementation [3]. While many parameters (e.g., architecture, materials) are known to affect  
39 MECs performances, anodic biofilm, as catalyser, is the fundamental parameter to be  
40 optimized for converting the electrons' flow to the electrode [4]. These biofilms are mostly  
41 composed of EABs able to use an anode as final electron acceptor [5]. Such electronic  
42 transfer can result from either a direct contact with the anode through redox active proteins  
43 (short range), or e-pili (long range), or an indirect transfer through soluble electronic shuttles  
44 [6]. During the oxidation of organic compounds (e.g., volatile fatty acids), it is necessary to  
45 maintain a low partial pressure of hydrogen or a low concentration of formate to make the  
46 chemical reactions thermodynamically favourable [7]. This implies a critical interdependence  
47 between a producer and a consumer, so, called syntrophy [8]. Thus, for a complete conversion  
48 of fermentable substrates (e.g., glucose, propionate, ethanol) to electrons, fermenters produce  
49 intermediate compounds such as hydrogen, formate or acetate which are then used by EABs  
50 to generate electrical current [9]. Some EABs such as *Geobacter metallireducens*, can even

51 convert directly fermentable substrates into electrons without syntrophic partners [10]. The  
52 numerous combinations of these interactions make the electroactive ecosystems still poorly  
53 understood.

54 One way to identify efficient anodic bacteria is to characterize the bacterial  
55 community composition of the anodic biofilms in relation to the MEC performances (CD &  
56 CE) [11]. Many substrate-specific EABs could potentially improve MECs performances.  
57 These EABs are efficient because they significantly contribute to the conversion of specific  
58 substrates into current. A great diversity is commonly observed together with the  
59 predominance of EABs or others metal-reducing bacteria [12, 13]. Among the already well  
60 known EABs, *Geobacter sulfurreducens* is often found dominant in ecosystems fed with  
61 either acetate or lactate as sole electron donor [14, 15]. Concerning propionate, the presence  
62 of *Geovibrio ferrireducens* was revealed by DGGE in microbial fuel cell (MFC) [16]. In the  
63 same study, *Pelomonas saccharophila* was found as major DGGE-band when butyrate was  
64 the sole electron donor. However, little information exists in the literature on the microbial  
65 structure of bioanodes.

66 The objective of this study was to determine the selection of substrate-specific  
67 microbial communities in MECs and bacteria directly related to electron fluxes. For that, four  
68 different substrates, acetate, lactate, propionate and butyrate were separately used as sole  
69 electron donor in quadruplicate. Indeed they are the main breakdown products produced by  
70 fermentative bacteria in wastewater treatment [17].

## 71 **2 Materials & Methods**

### 72 *2.1 Inoculum*

73 The microbial inoculum used in this work was sampled from the aeration tank of the  
74 Narbonne wastewater treatment plant (11100, France). The latter was freshly used without  
75 storage at 10% v/v.

### 76 *2.2 Operating of the MECs*

77 All chemicals were of analytical or biochemical grade and were purchased from Sigma-  
78 Aldrich. All potentials provided in this manuscript refer to the SCE reference electrode (KCL  
79 3.0 M, +240 mV vs. SHE, Materials Mates, La Guilletière 38900 Sarcenas, France). All  
80 media prepared were adjusted to pH=7, flushed with high-purity N<sub>2</sub> gas (purity ≥ 99.995 %,  
81 Linde, France) for at least 30 min using air injection cannula. Bioelectrochemical experiments  
82 were conducted under potentiostatic control (BioLogic Science Instruments, France) with EC-  
83 Laboratory v.10.1 software and strictly anaerobic. All incubations were placed in a water bath  
84 at 37°C. A magnetic stirrer rotating a 350 rpm to homogenize the mixture. MEC tests were  
85 performed in quadruplicate with anodic potential fixed at +210 mV vs SCE.

### 86 *2.3 Microbial electrolysis cell set up*

87 The electrochemical system used for this experiment corresponded to a two-chambers  
88 cylindrical microbial electrolysis cell to avoid the diffusion of hydrogen from the cathode to  
89 the anodic compartment. Each chamber had a working volume of 900 mL. The anode was  
90 composed of a 2.5 cm x 2.5 cm x 0.12 cm carbon plate (Mersen S.A, France), screwed onto a  
91 2-mm diameter titanium rod (T1007910/13, Goodfellow SARL, France). The cathode was  
92 made of a plate of 16 cm<sup>2</sup> of 90% Platinum and 10% Iridium mesh (Heraeus PSP., France).  
93 The MECs were hermetically sealed with silicone and stainless steel ring at each chamber.  
94 Both chambers were separated with an anion exchange membrane (AEM, Fumasep FAA,  
95 FuMA-Tech BWT GmbH, Germany). Batch was the operational mode for each experiment.

96 When the current density ( $A \cdot m^{-2}$ ) is close to half the maximum current density, the MEC has  
97 been stopped and the electroactive biofilm collected. This value was chosen to sample a still  
98 active biofilm.

#### 99 2.4 *MEC Medium*

100 The medium in the anodic chamber (per litre of water) was as follows: 0.5 g K<sub>2</sub>HPO<sub>4</sub>, 2.0 g  
101 NH<sub>4</sub>Cl, 7.6 g MES buffer, 0.2 g yeast extract, 12.5 mL trace metal element solution 141  
102 (DSMZ), 2.11 g Sodium 2-bromoethanesulfonate (2-BES) to inhibit methanogens. The  
103 cathodic medium (per liter of water) contained 0.5 g K<sub>2</sub>HPO<sub>4</sub>, 7.6 g MES buffer and 12.5 mL  
104 trace metal element solution 141 (DSMZ). Acetate, lactate, propionate and butyrate were  
105 separately used in anodic compartment as unique electron donor at a concentration of ~80 m  
106 e<sup>-</sup> eq.

#### 107 2.5 *Analytical Methods*

108 Concentrations of acetate, propionate, butyrate and lactate were measured by HPLC with a  
109 refractive index detector (Waters R410). First, samples were centrifuged at 13,500g for 15  
110 min and then supernatants were filtered with 0.2 µm syringe filter. HPLC analysis was  
111 performed at a flow rate of 0.4 mL/min on an Aminex HPX-87, 300 x 7.8 mm (Bio-Rad)  
112 column at 35°C with H<sub>2</sub>SO<sub>4</sub> (4 mM) as mobile phase. For each batch, the planktonic part was  
113 sampled after inoculation as the starting point, constituting the inoculum samples. At the end  
114 of each batch, the planktonic part was collected and constituted the bulk samples and the  
115 anodic biofilm was harvested with a blade. These three types of samples (Inocula, bulks and  
116 biofilms) were centrifuged at 13,500g for 15 min and the pellet was stored at -20°C prior to  
117 microbial community analyses.

118

## 119 2.6 *Microbial Community Analysis*

120 DNA extraction was carried out with QIAamp fast DNA stool mini kit in accordance with the  
121 manufacturer's instruction (Qiagen, Hilden, Germany). DNA extraction was confirmed using  
122 Infinited 200 PRO Nanoquant (Tecan Group Ltd., Männedorf, Switzerland). Amplicons from  
123 the V3 to V4 regions of 16S rRNA genes were amplified with bacterial forward 343F 5'-  
124 TACGGRAGGCAGCAG-3'; (Liu et al., 2007) and reverse 784R 5'-  
125 TACCAGGGTATCTAATCC-3'; (Anderson et al., 2008) primers. Adapters were added for  
126 multiplexing samples during the second amplification step of the sequencing. The PCR  
127 mixtures (50 µl) contained 0.5 U of Pfu Turbo DNA polymerase (Stratagene) with its  
128 corresponding buffer, 0.5 mM of each primer, 200 mM of each dNTP and 10 ng of genomic  
129 DNA. Reactions were carried out in a Mastercycler thermal cycler (Eppendorf) as follows:  
130 94°C for 2 min, followed by 35 cycles of 94°C for 1 min, 65°C for 1 min, and 72°C for 1 min  
131 and a final extension at 72°C for 10 min. The size and amount of PCR products were  
132 measured using a Bioanalyser 2100 (Agilent). The community composition was evaluated  
133 using the MiSeq v3 chemistry (Illumina) with 2 x 300 bp paired-end reads at the Genotoul  
134 platform ([www.genotoul.fr](http://www.genotoul.fr)). Sequences were retrieved after demultiplexing, cleaning, and  
135 affiliating using Mothur [18]. All sequences were submitted to Genbank under accession  
136 numbers MG238597 - MG241108.

## 137 2.7 *Quantitative PCR (qPCR)*

138 PCRs were prepared using 96-well real time PCR plates (Eppendorf, Hamburg, Germany) and  
139 Mastercycler ep gradient S (Eppendorf, Hamburg, Germany). After, 6.5 µl of Express qPCR  
140 supermix with premixed ROX (Invitrogen, France), 2 µl of DNA extract with three  
141 appropriate dilutions, 100 nM forward primer F338-354 (5'-ACTCCTACGG GAGGC AG-  
142 3'), 250 nM reverse primers R805-785 (5'-GACTA CCAGG GTATC TAATC C-3'), 50 nM

143 TaqMan probe and water were added to obtain a final volume of 12.5  $\mu$ l for all analyses. A  
144 first incubation of 2 min at 95°C followed by 40 cycles of denaturation (95°C, 7 s; 60°C, 25 s)  
145 was performed. From each assay, one standard curve was generated by using tenfold dilution  
146 in sterilized water (Aguettant Laboratory, Lyon, France) of a target plasmid (Eurofins  
147 Genomics, Germany). The initial DNA concentrations were quantified using the Infinite 200  
148 PRO NanoQuant (Tecan, France).

## 149 2.8 *Electron balances*

150 To estimate the electronic balances in each experiment, the distribution of electron in milli  $e^-$   
151 equivalent (m  $e^-$  eq) in the MECs was monitored by determining the electron donor  
152 conversion (acetate, propionate, lactate and butyrate) to various electron sinks (current,  
153 propionate, acetate, lactate, butyrate). Coulombic efficiency (CE) was estimated as the  
154 percentage of electrons that have passed through the circuit in a single batch test divided by  
155 the amount of electrons available after substrate oxidation [1].

156

## 157 2.9 *Statistical Analysis*

158 All statistical analyses were carried out in R version 3.2.3 (R core Team 2014). The  
159 differences between current densities and coulombic efficiencies between the conditions were  
160 tested with one-way ANOVA followed by Tuckey's HSD post-hoc test with a statistical  
161 significance ( $P$ -value)  $< 0.05$ ). Weighted-UniFrac distance-based PCoA ordination was used  
162 to represent inter-samples distances with phyloseq package [19]. The Monte Carlo simulation  
163 showed significant difference between microbial composition according to the substrates and  
164 sample types (Inocula, Bulks and Biofilms) with  $P$ -value of 0.001.

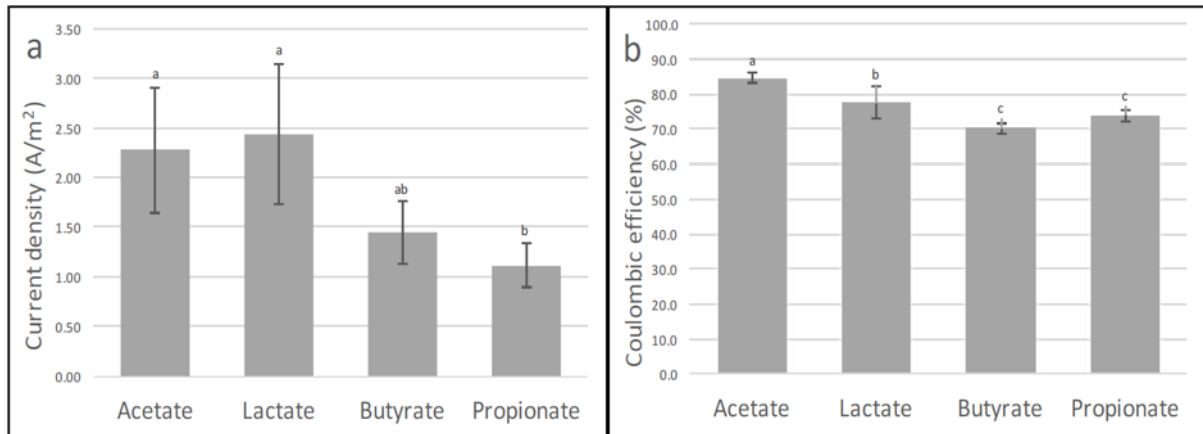
165

## 166 **3 Results & discussion**

### 167 *3.1 Influence of single substrates on coulombic efficiency and current density*

168 First, MECs performances were substantially influenced by the type of substrate.  
169 Regarding the current density (average of the maximum current densities), acetate- and  
170 lactate-fed MECs were the most efficient systems with a current density of  $2.28 \pm 0.62$  and  
171  $2.44 \pm 0.71 \text{ A.m}^{-2}$  respectively, in contrast to butyrate and propionate fed-MECs ( $1.45 \pm 0.32$   
172 and  $1.11 \pm 0.22 \text{ A.m}^{-2}$  respectively) (Fig. 1 – a). From these results, it was concluded that  
173 acetate and lactate were more rapidly converted into current. Acetate is a substrate which  
174 commonly produces high current densities in mixed cultures [2]. Since acetate accumulated  
175 after lactate fermentation (concomitantly with propionate, Fig. 5), it was not surprising to  
176 find similar current densities between acetate- and lactate-fed MECs. As observed in other  
177 studies, propionate and butyrate-fed MECs had the lowest current densities [13, 20].  
178 In terms of coulombic efficiencies (CE), (average of the 4 MECs per substrate), acetate-fed  
179 MECs showed the highest values ( $84.7 \pm 1.43\%$ ) as widely observed in other studies (Fig. 1 –  
180 b) [16, 21]. Lactate-fed MECs had an average CE of  $77.5 \pm 4.55 \%$ , indicating efficient  
181 electron recovery, probably due to the production of acetate as main fermentative product.  
182 Propionate- and butyrate-fed MECs had no-significant difference with respect to the CE ( $74.6$   
183  $\pm 1.72$  and  $70.2 \pm 1.49$  respectively). Based on these results, it appears that acetate was  
184 effectively converted to current. However, the addition of 2-BES that inhibits electron leakage  
185 to methane improved the coulombic efficiency for all the substrates tested in this study.





186

187 **Fig. 1** Performance of MECs (average of the batch cycles of the duplicate (n=4) reactors in term of a current  
 188 density of the maximum current density and b coulombic efficiency. Samples with the same letter (a, b or c)  
 189 have no significant difference.

190

### 191 3.2 Electron distribution at the end of the batch experiments

192 Except for lactate-MECs, electron balance at the end of the batch tests revealed that current  
 193 was the main electron sink (Table 1). Metabolite concentrations over time are shown in Fig. 5  
 194 & Fig.S 1-3. Nevertheless, most of the electrons remain present in the substrates (except for  
 195 lactate), since the experiments were stopped when the current density was decreasing and  
 196 close to half of the maximum peak. Concerning the lactate-fed MECs, the main end product  
 197 was propionate  $59.16 \pm 9.34$  %. This metabolite, together with acetate, is a co-product of the  
 198 lactate fermentation. No significant difference was observed between all conditions probably  
 199 due to a high intra-sample variability (standard deviation, Fig. 1-b) and the addition of  
 200 methanogenesis inhibitor (2-BES) which prevents electron leakage to methane.

201 Table 1

202 Distribution of electrons at the end of the MEC batch experiments in quadruplicate. 100% = initial electron  
 203 content in the substrates.

Electron sinks	Fraction of electrons at the end of MECs tests (%)			
	MECs Acetate	MECs Lactate	MECs Propionate	MECs Butyrate
Current	$37.21 \pm 14.34$	$31.88 \pm 4.2$	$30.13 \pm 6.02$	$34.36 \pm 13.68$
Acetate	$56.24 \pm 17.09$	-	-	-

Propionate	-	59.17 ± 8.24	59.16 ± 9.34	-
Butyrate	-	-	-	51.20 ± 11.21
Unknown sinks	6.54 ± 2.34	8.94 ± 2.00	10.76 ± 3.33	14.43 ± 6.42

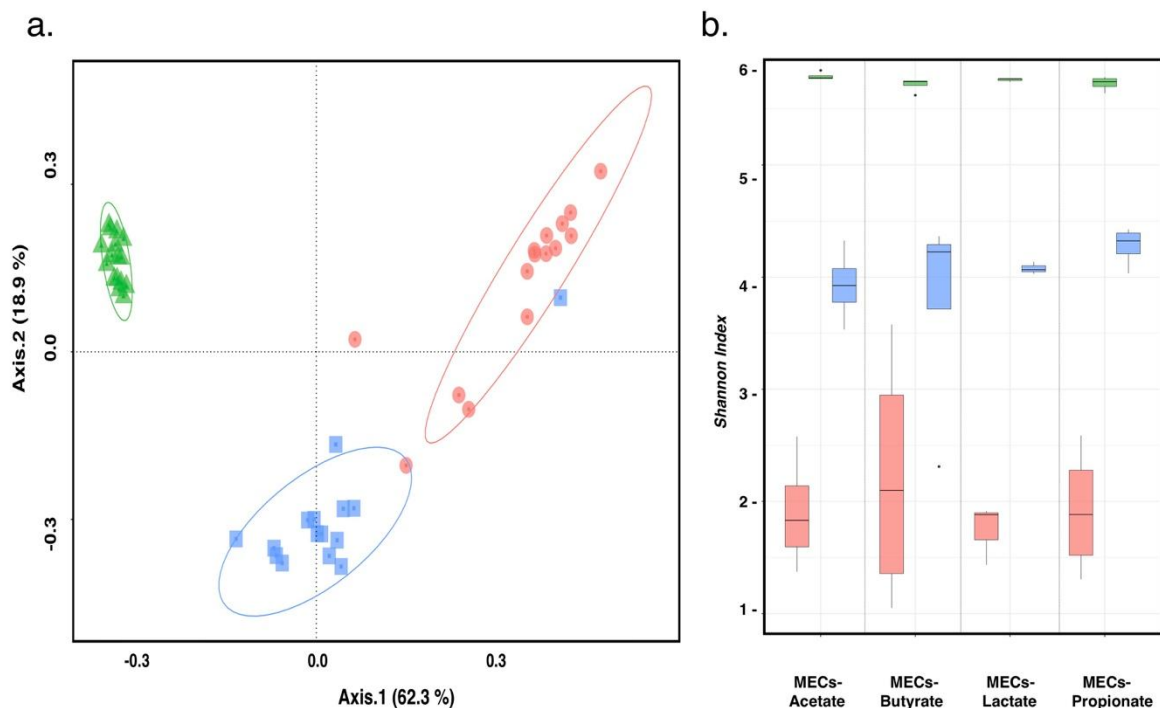
204

### 205 3.3 Analysis of the microbial communities

#### 206 3.3.1 Microbial diversity analysis

207 Principal Coordinate Analysis (PCoA) based on weighted-UniFrac distance matrix was used  
208 to represent the differences of microbial communities between the inoculum (corresponding  
209 to the ‘bulks’ at the beginning of each batch test) and the anode and bulk samples. Three clear  
210 and significantly distinct clusters ( $P$ -value < 0.05) regardless to the electron donor are  
211 observed in the PCoA plot (Fig. 2-a). Axis 1 represents 62.3% of the variance and allows to  
212 distinguish inocula, biofilms and bulks while axis 2 represents 18.9% of the total variance. To  
213 determine the differences in diversity between these three clusters and the electron donors, a  
214 Shannon index was calculated (Fig. 2-b). The Shannon index gives access to the specific  
215 diversity of each samples according to the number of species (species richness) and their  
216 distribution (specific equitability). Among the three clusters (Fig. 2-a), a significant  
217 difference was found between the Shannon indexes of the inocula, which had the highest  
218 diversity ( $5.57 \pm 0.03$ ), the bulks samples, having an average diversity ( $4.03 \pm 0.22$ ), and the  
219 anodic biofilms which had the lowest diversity ( $1.96 \pm 0.16$ ) whatever the substrate. The  
220 Butyrate-4 bulk sample had the lowest bulks’ diversity (Fig. 2-a) which likely explained its  
221 presence close to biofilm’s cluster on PCoA plot (Fig. 2-b). Moreover, the amount of 16S  
222 rRNA copies number, that is related to the cell number in each sample, is presented in Fig. 3.  
223 Here, inocula samples contained the highest copy numbers with an average of  
224  $2.95 \cdot 10^{12} \pm 3.69 \cdot 10^{11}$  copies of the 16S rRNA gene. At the end of experiments in bulks a  
225 significant decrease of the 16S rRNA copies number ( $1.83 \cdot 10^{11} \pm 1.28 \cdot 10^{11}$ ) was observed,

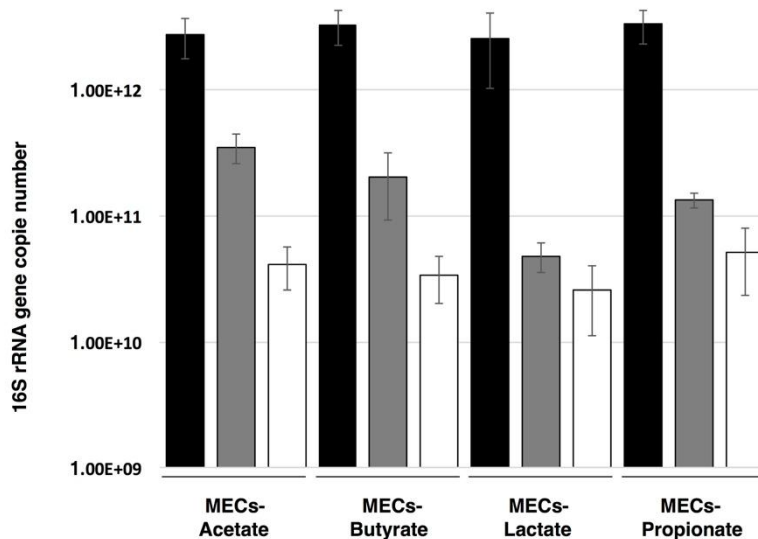
226 which indicates a cell mortality, probably due to the lack of soluble electron acceptors. Under  
 227 these conditions, only some taxa were able to survive, which could explain the decline of the  
 228 microbial diversity over time (Fig. 2-b). Concerning the biofilm samples, a number of  
 229  $3.78 \cdot 10^{10} \pm 1.08 \cdot 10^{10}$  16S rRNA copies was observed at the end of the experiments. This  
 230 clearly indicate a cellular growth on the anodic surface. The low diversity of the biofilms  
 231 ( $1.96 \pm 0.16$ ) compared to the bulks ( $4.03 \pm 0.22$ ), suggests that the growth was very selective.  
 232 Therefore, the anode appears to be a very selective ecological niche for bacterial  
 233 communities, probably due to the specific ability to form a biofilm and extracellular electron  
 234 transfer to grow, both of which being two important ecological factors that lead to a  
 235 significant decrease in diversity.



236

237 **Fig. 2** a. Principal coordinate analysis (PCoA) based on weighted-UniFrac distance matrix showing the  
 238 microbial distribution pattern for all substrates between inocula (▲ green triangles), bulks (■ blue squares) and  
 239 biofilms (● red points) samples. Clusters were defined by significance difference calculated by the permutation  
 240 test ( $n=9999$ ,  $P.value=0.001$ ) b. Shannon index of microbial communities according to MECs-substrates and  
 241 sample types (■ Inocula, ■ Bulks and ■ Biofilms).

242



243

244 **Fig. 3** Average of qPCR measurements per sample types (Inocula ■, Bulks ■ and Biofilms □) in copie number  
 245 of 16S rRNA gene.

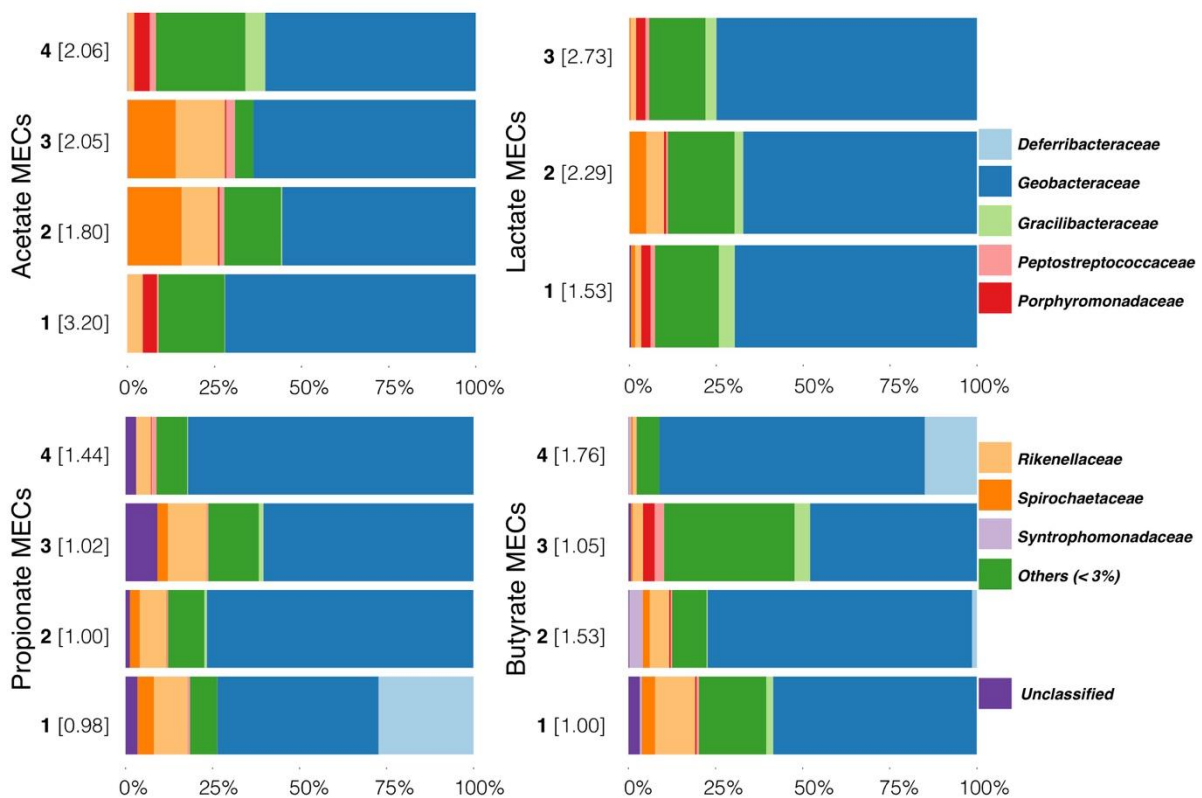
246

### 247 3.3.2 Anodic microbial communities according to the substrates

248 High-throughput sequencing of 16S rRNA gene was used to characterize the bacterial  
 249 communities of anodic biofilms and bulk samples from the sixteen MECs at the end of the  
 250 experiments. 16S rRNA gene library had 1,957,962 high-quality reads (average length ~404  
 251 bp) after treatment (denoising, quality filtering and removal of chimeric sequences). Lactate-4  
 252 sample, composed of OTUs present at less than 3% was excluded from the analysis due to  
 253 poor read sequencing quality. The sequences were assigned to OTUs with a  $\geq 95\%$  sequence  
 254 identity threshold. The classification with sequence identity of the bacterial communities is  
 255 provided in Supplementary Information (Table S 1).

256 All biofilms whatever the substrate were dominated by members of the *Geobacteraceae*  
 257 family, representing 62.41% of biofilms' sequences (Fig. 4). The *Rickenelaceae* family was  
 258 also present in all biofilms samples at 10.89% and 12.61% in propionate-3 and acetate-3  
 259 MECs respectively. This family is represented by the *Blvii28* wastewater sludge group (OTU  
 260 9 & 54), known to be strict anaerobic fermenters [22]. The *Deferribacteraceae* family is

261 mainly present in 2 samples, propionate-1 and butyrate-4 at 25.87% and 14.23% abundance  
 262 respectively. This family is represented by *Selenovibrio woodruffi* (OTU 15). Interestingly, *S.*  
 263 *woodruffi* can only use acetate as electron donor [23]. To explain its presence in biofilms, it  
 264 could be involved in acetate oxidation generated by propionate or butyrate fermentation by  
 265 syntrophic interactions. Selenate and arsenate, its known terminal electrons acceptors, are not  
 266 available in the culture media. Therefore, it would be interesting to determine whether this  
 267 bacterium has the ability to use the anode as final electron acceptor. The ‘Others’ category  
 268 represents all OTUs with an abundance of less than 3% in all biofilms.



269

270 **Fig. 4** Relative taxa abundances at Family level in anodic biofilms by MECs-type. Numbers (1-4) in bold are  
 271 specific to the replicate (except Lactate-MEC 4). Numbers in square brackets correspond to the peak current  
 272 density ( $A.m^{-2}$ ) of the sample.

273

### 274 3.3.3 Analysis of *Geobacter* species according to the substrates

275 As previously observed, the *Geobacteraceae* family was dominant in all biofilms.

276 Species of this family have a well-known metabolism with high capability of

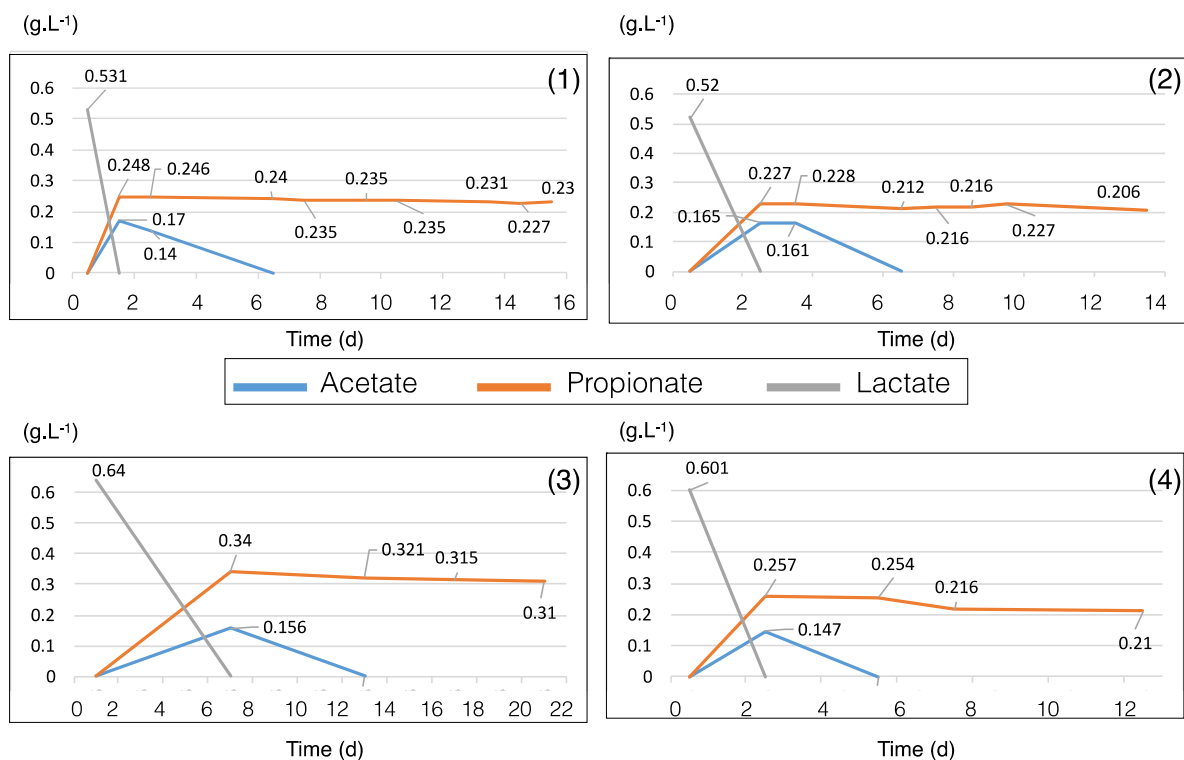
277 exoelectrogenesis [24]. For better understanding the metabolic pathways and ecological  
278 interactions, the balance between *Geobacter* species was analysed. At this level, it showed a  
279 specific relative distribution according to the substrate within *Geobacter* species (Fig. 6).

280 *Geobacter sulfurreducens* (OTU 1) was the main *Geobacter species* in acetate, lactate  
281 and butyrate-fed MECs (except Butyrate-4) with a balance of  $96.03 \pm 6.1\%$ ,  $95.84 \pm 4.4\%$  and  
282  $64.55 \pm 30\%$  respectively. This species was also present at 39.80% in Propionate-3 MEC.  
283 *Geobacter toluenoxydans* (OTU 2) was dominant in propionate-fed MECs (except  
284 Propionate-3) at  $78.51 \pm 18\%$  and replicate-4 of butyrate-fed MEC (97.78%). *Geobacter*  
285 *metallireducens* (OTU 5) was the second most abundant species in Propionate-1 and -3 MECs  
286 ( $38.20 \pm 2\%$ ) and was also present at 9.33% and 21.24% in Acetate-4 and Butyrate-3 MEC  
287 respectively. *Geobacter pelophilus* (OTU 12) was dominant in Butyrate-1 sample (52.85%)  
288 and second most abundant in Butyrate-3 sample (23.53%) and at 7.05% in Lactate-2 MEC.

289  
290 These results suggest that when acetate was in solution as main substrate or co-product i.e.  
291 Acetate- and Lactate-fed MECs (Fig. 5 & Fig. S-1), *G. sulfurreducens* predominated within  
292 the *Geobacter* genus. Indeed, this EAB is a well-known electroactive microorganism able to  
293 oxidize formate, H<sub>2</sub>, lactate and acetate with the anode as sole terminal electron acceptor [25].  
294 It could therefore be directly involved in acetate oxidation at the anode. *G. pelophilus* and *G.*  
295 *metallireducens*, which are also able to convert acetate into current were found in a minority  
296 in Acetate- and Lactate-fed MECs [26, 27]. Consequently, with regard to acetate as electron  
297 donor, competitive relations likely took place for anode colonization within the *Geobacter*  
298 genus. The competitive property of *G. sulfurreducens* leading to its predominance in the  
299 ecosystem has also been observed in a synthetic consortium [28]. In lactate-fed MECs, acetate  
300 was quickly oxidized (~4-6 days) while propionate was not degraded (Fig. 5). As observed in  
301 Fig. 4, these biofilms were dominated by *Geobacteraceae* family where *G. sulfurreducens*

302 was predominant (Fig. 6). Since the latter is unable to oxidizing propionate, its presence  
303 caused a 'barrier effect' preventing the presence of other EABs able to oxidize propionate.  
304 Indeed, *G. toluenoxydans* was predominant with propionate as electron donor (and in  
305 Butyrate-4 MEC). It is able to oxidize many substrates such as acetate, propionate and  
306 butyrate by reducing ferrihydrite or ferric citrate [29]. The present OTU appears to be  
307 involved in propionate and butyrate conversion into current. Interestingly, the predominance  
308 of *G. sulfurreducens* in three butyrate-fed MECs (1-, 2- and 3-replicates) and Propionate-3  
309 MEC whereas it is unable to use these two substrates as electron donors suggests that, within  
310 these biofilms, syntrophic interactions occurred. Similarly, *G. pelophilus* was dominant and  
311 second most abundant in *Geobacter* genus in presence of butyrate (Butyrate-1 and 3 MECs).  
312 This species is able to use acetate, pyruvate, ethanol and formate as electron donors but not  
313 butyrate, which suggests a syntrophic relationship with butyrate-oxidizing bacteria such as *G.*  
314 *metallireducens* [27]. Moreover, the latter is also known to establish syntrophic relationships  
315 with other *Geobacter* species [30]. Concerning propionate-fed MECs, *G. metallireducens* was  
316 systematically found beside *G. toluenoxydans*. *G. metallireducens* seems to have reached a  
317 specialized ecological niche in the use of propionate in a multi-species exoelectrogenic  
318 biofilm community [28]. These two bacteria which use the same electron donor, propionate,  
319 could indicate a competitive relationship to the substrate with an unexplained predominance  
320 for *G. toluenoxydans*.

321



322

323 **Fig. 5** Metabolite concentrations (g.L<sup>-1</sup>) during lactate-fed MECs assays over time (d) according to the replicate  
 324 numbers (1-4).

325

### 326 3.3.4 Analysis of bacterial communities according to MEC performance

327 Within the same substrate and similar physicochemical conditions, differences in peak current  
 328 densities were observed (Fig. 4 & Fig. 6). It is therefore interesting to determine whether  
 329 these differences can be explained by the composition of the bacterial communities. By this  
 330 means, effective or ineffective species with respect to current densities can be determined.  
 331 Firstly, for acetate- and lactate-MECs, there was a difference of 56.25 and 56.04 % between  
 332 the highest and lowest performance in CDs respectively (Fig. 4). With these substrates, *G.*  
 333 *sulfurreducens* was dominant regardless of the CDs produced. Therefore, these differences  
 334 were probably due to other bacterial families. In Acetate-MECs, the most efficient reactor  
 335 (Acetate-1, 3.20 A.m<sup>-2</sup>) contains only 0.056% of *Spirochaetaceae* contrary to the least



336 efficient (Acetate-2, 1.80 A.m<sup>-2</sup>) which contained 15.54%. This family is represented by  
337 *Treponema caldarium* (OTU 8) which is not able of using acetate directly as an electron  
338 donor but can be an hydrogen scavenger in ecosystems by oxidizing H<sub>2</sub> with CO<sub>2</sub> to produce  
339 acetate via the Wood-Ljungdahl (acetyl-CoA) pathway [31]. It would therefore be interesting  
340 to better understand its role in bio-anode to explain its ecological relationships and why this  
341 species seems to be ineffective regardless of the CDs produced. Concerning lactate-MECs,  
342 there is no difference in bacterial composition depending on performance (Fig. 4). In this  
343 case, minority bacteria, not well characterized in these systems, could play a role according to  
344 CDs. For propionate-MECs, a difference of 68.05 % in CDs is observed within the  
345 quadruplicate, with on one side Propionate-4 sample producing 1.44 A.m<sup>-2</sup> and on the other  
346 side Propionate-1 to 3 close to 1 A.m<sup>-2</sup>. As with Acetate- and Lactate-MECs, these  
347 differences do not appear to be attributable to the *Geobacter* species distributions, as  
348 Propionate-4 and Propionate-2 contain a similar proportion of *G. toluenoxydans* (73 % and  
349 67.45 % respectively) with a difference of 69.44% in CDs. Similarly, bacterial families have  
350 similar proportions regardless of performance. So, as with lactate, the explanation could be  
351 due to minority bacteria.

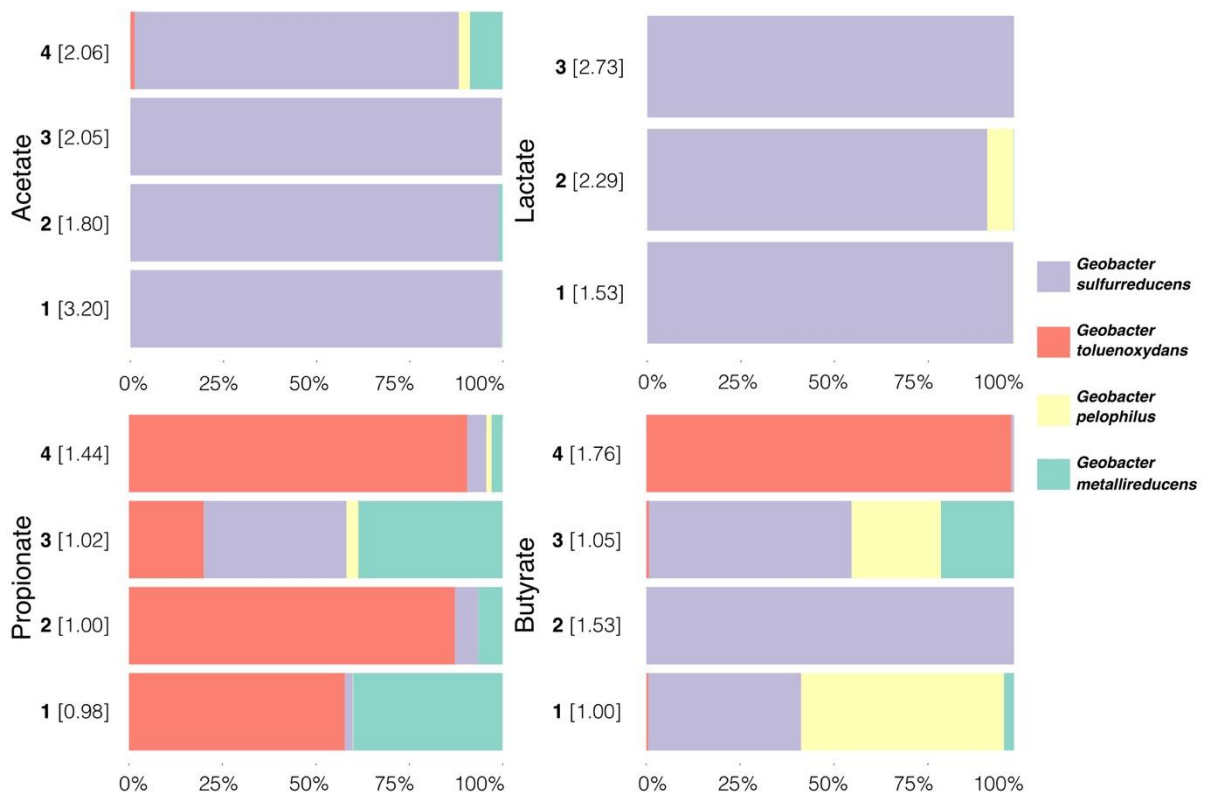
352 For butyrate-MECs, a difference of 56.81 % was observed between the most efficient reactor  
353 (Butyrate-4, 1.76 A.m<sup>-2</sup>) and the least efficient reactor (Butyrate-1, 1.00 A.m<sup>-2</sup>). In the  
354 *Geobacter* genus Butyrate-4 sample is composed of 74.58 % of *G. toluenoxydans* compared  
355 to Butyrate-1 (0.33 %). Thus, *G. toluenoxydans* could be an effective species for the  
356 conversion of butyrate to current and this seems to be consistent with its ability to use this  
357 metabolite directly, unlike the other OTUs mainly present in other biofilms (*G.*  
358 *sulfurreducens* & *G. pelophilus*) [29].

359

### 360 3.3.5 Hypothetical distribution of electrons from substrates to different electron sinks

361 In order to better understand the reasons why a bacterial species can increase (effective  
362 species) or decrease (ineffective species) the MEC performance, it is interesting to study the  
363 different hypothetical pathways involved in metabolite degradation. Based on experimental  
364 electron distribution, community analysis and bibliographic knowledge, the electron flux from  
365 the substrates could pass through various routes [11, 32]. Each route involves specific  
366 microbial communities such as fermenters, EABs and syntrophic hydrogenotrophs (EABs).  
367 The first possible route involved fermentation step with respect to lactate in the formation of  
368 propionate and acetate in a 2:1 molar ratio [33]. No fermentative metabolites were detected  
369 during experiments with propionate- and butyrate-fed MECs suggesting direct conversion  
370 (path 2) into current by EABs such as *G. toluenoxydans*. The third (acetate/H<sub>2</sub>) and four  
371 (formate) pathways are specific to syntrophic interactions. In the cases where they are not  
372 directly oxidized to current, the oxidation of fermentable substrates could produce  
373 intermediate metabolites which involved a microbial partnership between producers  
374 (acetate/H<sub>2</sub> or formate) such as *G. metallireducens* and consumers (i.e. EABs) such as *G.*  
375 *pelophilus* or *G. sulfurreducens* (Fig. 6). Thus, the oxidation of the previous substrates  
376 produces acetate/hydrogen (path 3) or formate (path 4) which can further be oxidized by  
377 syntrophic partners such as EABs to convert them into electricity [34]. A summary of the  
378 different possible routes can be seen in Schematic 1. The syntrophic pathway is less effective  
379 than the direct pathway, due to thermodynamic limitations to maintain low partial hydrogen  
380 pressure [35]. This is the reason why, depending on the species, the degradation pathways  
381 will be different (direct or indirect) which can impact the current densities. Experiments with  
382 synthetic bacterial consortia are necessary to validate these different hypotheses for a better  
383 understanding of the bacterial interactions.

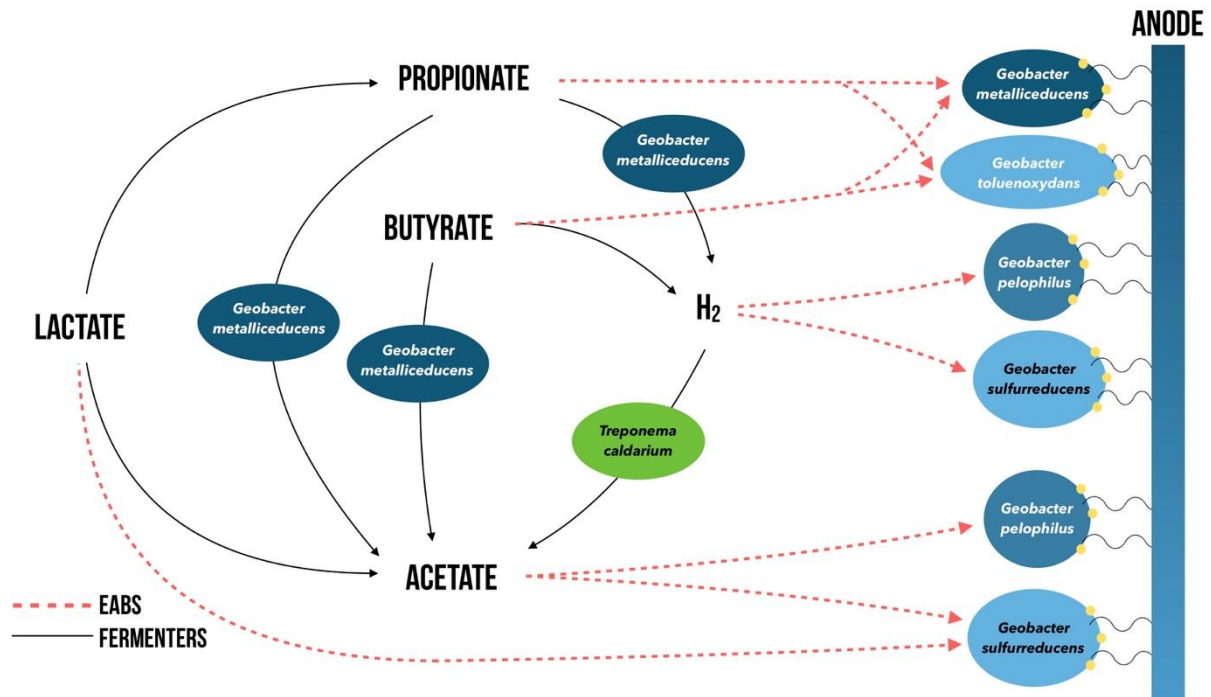
384



385

386 **Fig. 6** Relative abundances of the main *Geobacter* species found in the anodic biofilms according to the fed  
 387 substrate. The four *Geobacter* sp. represented 62.41% of total biofilm's sequences. Each *Geobacter* sp. is  
 388 identified by one specific colour. Numbers (1-4) in bold are specific to the replicate (except Lactate-MEC 4).  
 389 Numbers in brackets correspond to the maximum current density (A.m<sup>-2</sup>) of the sample.

390



391

392 **Schematic 1** Hypothetical degradation pathways of the substrates tested in this study associated with anodic  
 393 microorganisms mapping according to their metabolic potentials and abundances of community structures.

394

## 395 4 Conclusion

396 Lactate- and acetate-fed MECs showed higher performances in term of current densities and  
 397 coulombic efficiencies with regard to those fed with butyrate and propionate. The biofilms  
 398 diversity was the lowest when compared to bulks and inocula samples, indicating a selective  
 399 growth on anode as sole electron acceptor. Analysis of the microbial communities showed a  
 400 predominance of the *Geobacteraceae* family (62.41% of the total sequences) but a different  
 401 distribution at the *Geobacter* species-level according to the substrate. On the one hand *G.*  
 402 *sulfurreducens* appears to be involved in competitive relationships in presence of acetate  
 403 beside *G. metallireducens* and *G. pelophilus*. More complex substrates such as propionate and  
 404 butyrate appear to induce syntrophic interactions between acetate producers (e.g. *G.*

405 *metallireducens*) and consumers (e.g. *G. sulfurreducens* and *G. pelophilus*). Regarding the  
406 link between bacterial communities and performances, *Treponema caldarium* appears to be  
407 inefficient in the case of acetate oxidation, while *G. toluenoxydans* appears to be efficient for  
408 the conversion of propionate to current by its ability to use this metabolite directly without  
409 establishing syntrophy. Finally, these results allowing for the first time to make hypotheses of  
410 the ecological relationships existing within electroactive consortia as well as the ‘barrier  
411 effect’ that was probably caused by *G. sulfurreducens* and its low metabolic versatility  
412 preventing propionate oxidation. Consequently, it would be interesting to better understand  
413 the ‘barrier effect’ and the means to balance the electroactive ecosystems with propionate  
414 effective-species to promote propionate oxidation with acetate in solution.

## 415 **5 Acknowledgements**

416 This work was supported by a PhD Grant of Montpellier Sup Agro and funded by the French  
417 National Institute for Agricultural Research (INRA).

## 418 **6 References**

- 419 [1] B. E. Logan and K. Rabaey, "Conversion of wastes into bioelectricity and chemicals  
420 by using microbial electrochemical technologies," *Science*, vol. 337, no. 6095, pp. 686-90,  
421 Aug 10 2012.
- 422 [2] A. Wang *et al.*, "Integrated hydrogen production process from cellulose by combining  
423 dark fermentation, microbial fuel cells, and a microbial electrolysis cell," *Bioresour Technol*,  
424 vol. 102, no. 5, pp. 4137-43, Mar 2011.
- 425 [3] J. R. Trapero, L. Horcajada, J. J. Linares, and J. Lobato, "Is microbial fuel cell  
426 technology ready? An economic answer towards industrial commercialization," *Applied*  
427 *Energy*, vol. 185, pp. 698-707, 2017.

- 428 [4] N. S. Malvankar, J. Lau, K. P. Nevin, A. E. Franks, M. T. Tuominen, and D. R.  
429 Lovley, "Electrical conductivity in a mixed-species biofilm," *Appl Environ Microbiol*, vol. 78,  
430 no. 16, pp. 5967-71, Aug 2012.
- 431 [5] A. Tremouli, M. Martinos, S. Bebelis, and G. Lyberatos, "Performance assessment of  
432 a four-air cathode single-chamber microbial fuel cell under conditions of synthetic and  
433 municipal wastewater treatments," *Journal of Applied Electrochemistry*, vol. 46, no. 4, pp.  
434 515-525, 2016.
- 435 [6] D. R. Lovley, "Electromicrobiology," *Annu Rev Microbiol*, vol. 66, pp. 391-409, 2012.
- 436 [7] A. J. Stams and C. M. Plugge, "Electron transfer in syntrophic communities of  
437 anaerobic bacteria and archaea," *Nat Rev Microbiol*, vol. 7, no. 8, pp. 568-77, Aug 2009.
- 438 [8] B. E. Morris, R. Henneberger, H. Huber, and C. Moissl-Eichinger, "Microbial  
439 syntrophy: interaction for the common good," *FEMS Microbiol Rev*, vol. 37, no. 3, pp. 384-  
440 406, May 2013.
- 441 [9] P. Parameswaran, H. Zhang, C. I. Torres, B. E. Rittmann, and R. Krajmalnik-Brown,  
442 "Microbial community structure in a biofilm anode fed with a fermentable substrate: the  
443 significance of hydrogen scavengers," *Biotechnol Bioeng*, vol. 105, no. 1, pp. 69-78, Jan 01  
444 2010.
- 445 [10] B. E. Logan, "Exoelectrogenic bacteria that power microbial fuel cells," *Nat Rev*  
446 *Microbiol*, vol. 7, no. 5, pp. 375-81, May 2009.
- 447 [11] P. D. Kiely, J. M. Regan, and B. E. Logan, "The electric picnic: synergistic  
448 requirements for exoelectrogenic microbial communities," *Curr Opin Biotechnol*, vol. 22, no.  
449 3, pp. 378-85, Jun 2011.
- 450 [12] K. L. Lesnik and H. Liu, "Establishing a core microbiome in acetate-fed microbial fuel  
451 cells," *Appl Microbiol Biotechnol*, vol. 98, no. 9, pp. 4187-96, May 2014.

- 452 [13] K. J. Chae, M. J. Choi, J. W. Lee, K. Y. Kim, and I. S. Kim, "Effect of different  
453 substrates on the performance, bacterial diversity, and bacterial viability in microbial fuel  
454 cells," *Bioresour Technol*, vol. 100, no. 14, pp. 3518-25, Jul 2009.
- 455 [14] M. D. Yates *et al.*, "Convergent development of anodic bacterial communities in  
456 microbial fuel cells," *ISME J*, vol. 6, no. 11, pp. 2002-13, Nov 2012.
- 457 [15] S. Jung and J. M. Regan, "Comparison of anode bacterial communities and  
458 performance in microbial fuel cells with different electron donors," *Appl Microbiol*  
459 *Biotechnol*, vol. 77, no. 2, pp. 393-402, Nov 2007.
- 460 [16] S. Freguia, E. H. Teh, N. Boon, K. M. Leung, J. Keller, and K. Rabaey, "Microbial  
461 fuel cells operating on mixed fatty acids," *Bioresour Technol*, vol. 101, no. 4, pp. 1233-8, Feb  
462 2010.
- 463 [17] R. D. Cusick, P. D. Kiely, and B. E. Logan, "A monetary comparison of energy  
464 recovered from microbial fuel cells and microbial electrolysis cells fed winery or domestic  
465 wastewaters," *International Journal of Hydrogen Energy*, vol. 35, no. 17, pp. 8855-8861,  
466 2010.
- 467 [18] P. D. Schloss *et al.*, "Introducing mothur: open-source, platform-independent,  
468 community-supported software for describing and comparing microbial communities," *Appl*  
469 *Environ Microbiol*, vol. 75, no. 23, pp. 7537-41, Dec 2009.
- 470 [19] P. J. McMurdie and S. Holmes, "phyloseq: an R package for reproducible interactive  
471 analysis and graphics of microbiome census data," *PLoS One*, vol. 8, no. 4, p. e61217, 2013.
- 472 [20] H. Liu, S. Cheng, and B. E. Logan, "Production of Electricity from Acetate or  
473 Butyrate Using a Single-Chamber Microbial Fuel Cell," *Environmental Science &*  
474 *Technology*, vol. 39, no. 2, pp. 658-662, 2005.
- 475 [21] N. Yang, H. Hafez, and G. Nakhla, "Impact of volatile fatty acids on microbial  
476 electrolysis cell performance," *Bioresour Technol*, vol. 193, pp. 449-55, Oct 2015.

- 477 [22] X. L. Su *et al.*, "Acetobacteroides hydrogenigenes gen. nov., sp. nov., an anaerobic  
478 hydrogen-producing bacterium in the family Rikenellaceae isolated from a reed swamp," *Int J*  
479 *Syst Evol Microbiol*, vol. 64, no. Pt 9, pp. 2986-91, Sep 2014.
- 480 [23] I. Rauschenbach, V. Posternak, P. Cantarella, J. McConnell, V. Starovoytov, and M.  
481 M. Haggblom, "Seleniivibrio woodruffii gen. nov., sp. nov., a selenate- and arsenate-respiring  
482 bacterium in the Deferribacteraceae," *Int J Syst Evol Microbiol*, vol. 63, no. Pt 10, pp. 3659-  
483 65, Oct 2013.
- 484 [24] B. E. Logan and J. M. Regan, "Electricity-producing bacterial communities in  
485 microbial fuel cells," *Trends Microbiol*, vol. 14, no. 12, pp. 512-8, Dec 2006.
- 486 [25] A. M. Speers and G. Reguera, "Electron donors supporting growth and electroactivity  
487 of *Geobacter sulfurreducens* anode biofilms," *Appl Environ Microbiol*, vol. 78, no. 2, pp. 437-  
488 44, Jan 2012.
- 489 [26] P. L. Tremblay, M. Aklujkar, C. Leang, K. P. Nevin, and D. Lovley, "A genetic  
490 system for *Geobacter metallireducens*: role of the flagellin and pilin in the reduction of Fe(III)  
491 oxide," *Environ Microbiol Rep*, vol. 4, no. 1, pp. 82-8, Feb 2012.
- 492 [27] K. L. Straub and B. E. Buchholz-Cleven, "*Geobacter bremensis* sp. nov. and  
493 *Geobacter pelophilus* sp. nov., two dissimilatory ferric-iron-reducing bacteria," *Int J Syst Evol*  
494 *Microbiol*, vol. 51, no. Pt 5, pp. 1805-8, Sep 2001.
- 495 [28] A. Prokhorova, K. Sturm-Richter, A. Doetsch, and J. Gescher, "Resilience, Dynamics,  
496 and Interactions within a Model Multispecies Exoelectrogenic-Biofilm Community," *Appl*  
497 *Environ Microbiol*, vol. 83, no. 6, Mar 15 2017.
- 498 [29] U. Kunapuli, M. K. Jahn, T. Lueders, R. Geyer, H. J. Heipieper, and R. U.  
499 Meckenstock, "*Desulfitobacterium aromaticivorans* sp. nov. and *Geobacter toluenoxydans* sp.  
500 nov., iron-reducing bacteria capable of anaerobic degradation of monoaromatic  
501 hydrocarbons," *Int J Syst Evol Microbiol*, vol. 60, no. Pt 3, pp. 686-95, Mar 2010.



- 502 [30] P. M. Shrestha *et al.*, "Syntrophic growth with direct interspecies electron transfer as  
503 the primary mechanism for energy exchange," *Environ Microbiol Rep*, vol. 5, no. 6, pp. 904-  
504 10, Dec 2013.
- 505 [31] J. R. Leadbetter, T. M. Schmidt, J. R. Graber, and J. A. Breznak, "Acetogenesis from  
506 H<sub>2</sub> plus CO<sub>2</sub> by spirochetes from termite guts," *Science*, vol. 283, no. 5402, pp. 686-9, Jan 29  
507 1999.
- 508 [32] A. R. Hari, K. P. Katuri, E. Gorron, B. E. Logan, and P. E. Saikaly, "Multiple paths of  
509 electron flow to current in microbial electrolysis cells fed with low and high concentrations of  
510 propionate," *Appl Microbiol Biotechnol*, vol. 100, no. 13, pp. 5999-6011, Jul 2016.
- 511 [33] B. Schink, "Fermentation of 2,3-butanediol by *Pelobacter carbinolicus* sp. nov. and  
512 *Pelobacter propionicus* sp. nov., and evidence for propionate formation from C<sub>2</sub> compounds,"  
513 *Archives of Microbiology*, vol. 137, no. 1, pp. 33-41, 1984.
- 514 [34] P. Parameswaran, C. I. Torres, H. S. Lee, B. E. Rittmann, and R. Krajmalnik-Brown,  
515 "Hydrogen consumption in microbial electrochemical systems (MXCs): the role of homo-  
516 acetogenic bacteria," *Bioresour Technol*, vol. 102, no. 1, pp. 263-71, Jan 2011.
- 517 [35] D. Sun, D. F. Call, P. D. Kiely, A. Wang, and B. E. Logan, "Syntrophic interactions  
518 improve power production in formic acid fed MFCs operated with set anode potentials or  
519 fixed resistances," *Biotechnol Bioeng*, vol. 109, no. 2, pp. 405-14, Feb 2012.

520